A learning algorithm for the calibration of internal model uncertainties in advanced wind turbine controllers

A wind speed measurement-free approach

Mulders, S. P.; Brandetti, L.; Spagnolo, F.; Liu, Y.; Christensen, P.B.; Wingerden, J. W. van

DOI
10.23919/ACC55779.2023.10156125

Publication date
2023

Document Version
Final published version

Published in
Proceedings 2023 American Control Conference (ACC)

IEEE Control Systems Letters paper presented at
2023 American Control Conference (ACC)
San Diego, CA, USA. May 31 - June 2, 2023

A learning algorithm for the calibration of internal model uncertainties in advanced wind turbine controllers: A wind speed measurement-free approach

S.P. Mulders[1], L. Brandetti[1], F. Spagnolo[2], Y. Liu[1], P.B. Christensen[2] and J.W. van Wingerden[1]

Abstract— **Wind turbine partial-load controllers have evolved from simple static nonlinear function implementations to more advanced dynamic controller structures. Such dynamic control schemes have the potential to improve power production performance in realistic environmental conditions and allow for a more granular trade-off between loads and energy capture. The control structure generally consists of a wind speed estimator (WSE) combined with a controller aiming to track the commanded tip-speed ratio (TSR) reference. The performance and resulting closed-loop system stability are however highly dependent on the accuracy of the internal model in the WSE-TSR tracking scheme. Therefore, developing learning algorithms to calibrate the internal model is of particular interest. Previous works have proposed such algorithms; however, they all rely on the availability of (rotor-effective) wind speed measurements. For the first time, this paper proposes an excitation-based learning algorithm that exploits the closed-loop dynamic structure of the WSE-TSR tracking scheme. This algorithm calibrates the internal model without the need for wind speed measurements. Analysis and simulations show that the proposed algorithm corrects for model uncertainties in the form of magnitude scaling errors under ideal constant and realistic turbulent wind conditions.**

I. INTRODUCTION

In the past years, the global installed capacity of wind turbines has increased exponentially and is expected to increase further by 116 GW between 2022 – 2026 [1]. In July 2021, the European Commission presented a new 2030 climate target to increase the share of renewable energy sources to at least 40 %. To attain this goal, an average power capacity of 32 GW needs to be installed on a yearly basis. The most economically viable and efficient fashion of doing so for wind energy, is by deploying turbines with as high as possible power capacities [2]. For this reason, there is an ever-growing urge to further increase the turbine-rated power outputs, which consequentially demands even larger turbine sizes. Advanced and highly optimized wind turbine controllers can facilitate this development [3].

Nowadays, state-of-the-art control schemes combine a wind speed estimator and tip-speed ratio (WSE-TSR) tracking controller for partial-load region control. In contrast to the conventional standard $K\omega^2$ torque control strategy [4], the more advanced WSE-TSR tracking controller has the potential to improve power extraction performance, and provides a more granular trade-off between loads and energy capture [5][6]. In the WSE-TSR tracking scheme, the rotor-effective wind speed (REWS) estimate [7] is leveraged to calculate a rotor speed reference. The REWS is the wind speed corresponding to the kinetic energy flux through the total swept area of a wind turbine [8]. Then, to close the loop, the difference between the reference and the measured rotor speed is utilized as error feedback by the TSR tracking controller.

In [9], it is found that the WSE-TSR tracking scheme is inherently ill-conditioned by analysis using a control-oriented linear analysis framework. In the presence of model uncertainty, the problem of ill-conditioning inevitably leads to a biased effective wind speed estimate. As a consequence, the ill-conditioning causes the real-world wind turbine to deviate from the commanded operating point, possibly resulting in sub-optimal performance and/or stability issues.

A precise REWS estimate is thus highly dependent on the accuracy of the internal model parameters representing the actual aerodynamic properties of the wind turbine. However, these modeled parameters often initially already deviate significantly from the actual aerodynamic characteristics and tend to vary further over time due to, e.g., blade erosion and ice, residue, and bug build-up [10][11]. Therefore, to sustain control performance, calibration increasing the accuracy of the internal model is of special interest.

Various learning schemes have been proposed in the past. The work of [12] suggests reconstructing a calibrated power coefficient mapping with Gaussian process regression based on standard real-time turbine measurements. Another study describes an online method to estimate the power coefficient by measuring the wind speed, generator voltage, and current [13]. While the works provide solutions for the calibration of model information, they all assume and rely on the availability of (accurate) hub height or rotor-effective wind speed measurements. Because the wind is generally measured downwind by a point-wise hub-height anemometer, the assumption of sufficient accuracy of such a measurement is rather unrealistic considering the spatial variability of the wind over rotor swept area for large-scale turbines [7]. Moreover, there is an additional challenge in accurately computing power coefficient information from such measurements [14].

The current work proposes a novel learning algorithm that allows for calibrating the turbine model parameters without the need for a wind speed measurement. The algorithm

[1]Delft University of Technology, Delft Center for Systems and Control, Mekelweg 2, 2628 CD Delft, The Netherlands. {S.P.Mulders, L.Brandetti, Y.Liu-17, J.W.vanWingerden}@tudelft.nl.
[2]Vestas Wind Systems A/S, Hedeager 42, 8200 Aarhus N, Denmark.

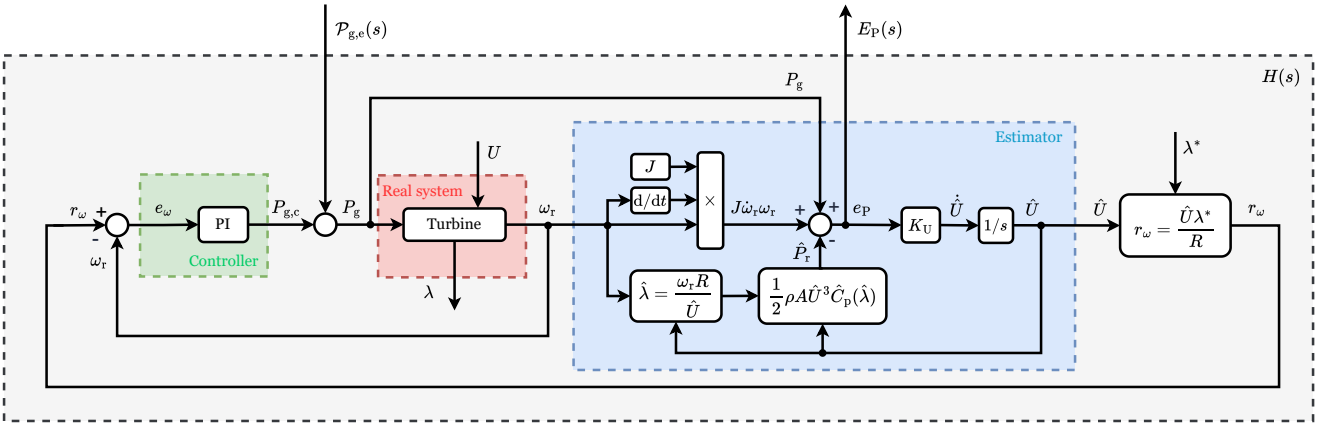

Fig. 1. Block diagram of the partial-load wind turbine controller. The red box contains the wind turbine system (model), with generator power set point P_g as control input, rotor speed ω_r as output, and subject to an REWS U disturbance. The wind speed estimator is indicated in blue and relies on the system in- and output, and a nonlinear internal model of the wind turbine to compute a rotor-effective wind speed estimate $\hat{U}$. This estimate is subsequently used to compute the rotor speed set point r_ω. This set point is used to calculate error e_ω by subtracting the actual rotor speed ω_r, which is provided as an input to the PI controller indicated in green. The controller provides the generator power set point P_g.

exploits the inherent dynamic structure of the WSE-TSR tracking controller by excitation of the closed-loop system and real-time calibration of the internal model information. This paper presents the following contributions:

1) Demonstrating that the magnitude response of a specific input-output (I/O) pair of the closed-loop system possesses convex properties with diminishing uncertainty of the internal model.
2) Providing a frequency-domain analysis framework for the interpretation and analysis of the convex properties.
3) Proposing an excitation-based learning algorithm for calibrating the internal control model.

The paper is organized as follows. Section II presents the WSE-TSR tracking scheme considered in this paper. By deriving a linear frequency-domain analysis framework, the scheme is shown to possess remarkable properties for a specific I/O pair in its transfer. Next, Section III presents the convex properties when the scheme is subject to model uncertainty. Section IV outlines the proposed learning algorithm that takes advantage of these convex properties. Section V showcases simulation results on the learning process. Finally, conclusions are drawn in Section VI.

PREREQUISITES

Functions of values indicating the modeled and/or intended optimal parameters are presented with $(\cdot)^\diamond$, whereas estimated quantities and uncertain modeled information in the estimator and/or controller are indicated by $\hat{(\cdot)}$. Demodulated signals at a specific frequency ω are presented with $\breve{(\cdot)}$.

Furthermore, this work relies on a collection of assumptions, which are summarized in this section. It is possible to alleviate some of the assumptions, however, the focus of this paper is to expose the key working principles of the learning algorithm in a clear and concise fashion.

Assumption 1. *The turbine is assumed to only operate in the partial-load region subject to generator power control, at a constant (fine) pitch angle. Therefore, the power coefficient information is only taken as a function of the tip-speed ratio.*

Assumption 2. *Among all the modeled parameters in the WSE-TSR tracking scheme, only the power-coefficient information is assumed to be uncertain.*

Assumption 3. *An element-wise function multiplication induces power coefficient uncertainty for the entire domain of the power-coefficient array.*

Assumption 4. *The rotor speed acceleration, which is in practical scenarios often estimated or computed numerically, is assumed to be an available and exact signal to the wind speed estimator.*

II. THEORY AND DERIVATIONS

This section presents the WSE-TSR tracking scheme that is considered throughout this paper. Furthermore, the system is linearized for the frequency-domain analysis of a particular input-output combination of interest. The considered transfer turns out to possess enabling properties for the development of the learning algorithm.

A. Time-domain representation

This section provides a derivation of the advanced wind turbine control scheme, consisting of a combined rotor-effective wind speed estimator and a controller tracking a constant tip-speed ratio. Fig. 1 presents a block diagram of the WSE-TSR tracking controller. Only the main results of the distinct elements in the scheme are given in this work; the reader will be referred to other works for more extensive derivations.

The wind turbine system is modeled as a first-order system

$$J\dot{\omega}_r(t)\omega_r(t) = P_r(t) - P_g(t), \tag{1}$$

in which $J \in \mathbb{R}$ is the effective rotor inertia converted to the low-speed shaft (LSS), $\omega_r \in \mathbb{R}$ is the rotor speed, and $P_r \in \mathbb{R}$ and $P_g \in \mathbb{R}$ are the respective aerodynamic power and

generator power set point, the latter of which is assumed to be directly related to the generator power. The time indication t is from this point omitted, unless its inclusion improves in clarity. The aerodynamic power is given by

$$P_{\mathrm{r}} = \frac{1}{2}\rho A U^3 C_{\mathrm{P}}(\lambda), \tag{2}$$

where $\rho \in \mathbb{R}$ is the fluid (air) density, $A \in \mathbb{R}$ the rotor swept area, $U \in \mathbb{R}$ the rotor effective wind speed, and $C_{\mathrm{P}} : \mathbb{R} \to \mathbb{R}$ the rotor power coefficient mapping as a function of the dimensionless tip-speed ratio

$$\lambda = \omega_{\mathrm{r}} R / U, \tag{3}$$

with R being the rotor radius (Assumption 1).

The employed wind speed estimator is a dynamic variant of the commonly applied power (or torque) balance equation [5], and has a high degree of similarity with the immersion and invariance (I&I) estimator [15][16], and is given by

$$\dot{\hat{U}} = K_{\mathrm{U}} e_{\mathrm{P}} = K_{\mathrm{U}} \left(P_{\mathrm{g}} - \hat{P}_{\mathrm{r}} + J \dot{\omega}_{\mathrm{r}} \omega_{\mathrm{r}} \right), \tag{4}$$

where K_{U} is the estimator gain, and the estimated aerodynamic rotor power is defined as

$$\hat{P}_{\mathrm{r}} = \frac{1}{2}\rho A \hat{U}^3 \hat{C}_{\mathrm{P}}(\hat{\lambda}), \tag{5}$$

with $\hat{\lambda} = \omega_{\mathrm{r}} R / \hat{U}$. The tip-speed ratio tracking controller is a proportional-integral (PI) controller

$$\dot{P}_{\mathrm{g}} = K_{\mathrm{p}} \dot{e}_{\omega} + K_{\mathrm{i}} e_{\omega}, \tag{6}$$

in which the error $e_{\omega} = r_{\omega} - \omega_{\mathrm{r}}$ is the respective difference between the rotor speed and the time-varying rotor speed set point $r_{\omega}(t)$, which is obtained based on (3) with the desired tip-speed ratio λ^* and the estimated wind speed $\hat{U}$.

B. Frequency-domain representation

With the time-domain representations of all the elements at hand, this section provides various open- and closed-loop frequency domain transfer functions that will appear to be useful in the remainder of this paper.

First the open-loop wind turbine with wind speed estimator in series is derived. To this end, the state is defined as $\mathbf{x} = \begin{bmatrix} \omega_{\mathrm{r}}, & \hat{U} \end{bmatrix}^{\mathrm{T}}$, the input $\mathbf{u} = [P_{\mathrm{g,e}}, \ P_{\mathrm{g,c}}]^{\mathrm{T}}$ consists out of a respective excitation and controller power contribution, and the output is defined as $\mathbf{y} = g(\mathbf{x}, \mathbf{u}) = [e_{\omega}, \ e_{\mathrm{P}}]^{\mathrm{T}}$. Thereby, taking into account Assumption 4, the following nonlinear state-space state equation is proposed

$$\dot{\mathbf{x}} = f(\mathbf{x}, \mathbf{u}) = \begin{bmatrix} 1 / \left(J \omega_{\mathrm{r}} \right) \left(P_{\mathrm{r}} - P_{\mathrm{g}} \right) \\ K_{\mathrm{U}} \left(P_{\mathrm{g}} - \hat{P}_{\mathrm{r}} + J \dot{\omega}_{\mathrm{r}} \omega_{\mathrm{r}} \right) \end{bmatrix}. \tag{7}$$

Linearizing the above-given equations by taking the Jacobian with respect to the state, input, and output vectors results in

$$\mathbf{A} = \begin{bmatrix} \left(T + \bar{P}_{\mathrm{g}} / \bar{\omega}_{\mathrm{r}}^2 \right) / J & 0 \\ K_{\mathrm{U}} \left(Q - \hat{Q} \right) & -K_{\mathrm{U}} V \end{bmatrix}, \ \mathbf{B} = \frac{-1}{J \bar{\omega}_{\mathrm{r}}} \begin{bmatrix} 1 & 1 \\ 0 & 0 \end{bmatrix}, \tag{8}$$

$$\mathbf{C} = \begin{bmatrix} 1 & -\lambda^* / R \\ \left(Q - \hat{Q} \right) & -V \end{bmatrix}, \qquad \mathbf{D} = \mathbf{0}, \tag{9}$$

where $Q = \partial P_{\mathrm{r}} / \partial \omega_{\mathrm{r}}$, $\hat{Q} = \partial \hat{P}_{\mathrm{r}} / \partial \omega_{\mathrm{r}}$, $T = \partial \tau_{\mathrm{r}} / \partial \omega_{\mathrm{r}}$, and $V = \partial \hat{P}_{\mathrm{r}} / \partial \hat{U}$. A unique transfer function representation of the state-space system in (8)–(9) is obtained using $\mathbf{C}(s\mathbf{I} - \mathbf{A})^{-1}\mathbf{B} + \mathbf{D}$, resulting in

$$\mathbf{G}(s) = \begin{bmatrix} G_{1,1}(s) & G_{1,2}(s) \\ G_{2,1}(s) & G_{2,2}(s) \end{bmatrix} = \begin{bmatrix} G_1(s) & G_1(s) \\ G_2(s) & G_2(s) \end{bmatrix}, \tag{10}$$

where s is the Laplace operator, and

$$G_1(s) = \frac{-1}{J \bar{\omega}_{\mathrm{r}}} \left(\frac{s + K_{\mathrm{U}} \left(V - \lambda^* / R \left(Q - \hat{Q} \right) \right)}{\left(s - \left(T + \bar{P}_{\mathrm{g}} / \bar{\omega}_{\mathrm{r}}^2 \right) / J \right) \left(s + K_{\mathrm{U}} V \right)} \right),$$

$$G_2(s) = \frac{-1}{J \bar{\omega}_{\mathrm{r}}} \left(\frac{\left(Q - \hat{Q} \right) s}{\left(s - \left(T + \bar{P}_{\mathrm{g}} / \bar{\omega}_{\mathrm{r}}^2 \right) / J \right) \left(s + K_{\mathrm{U}} V \right)} \right).$$

By defining the transfer function for the PI controller as

$$C(s) = \frac{P_{\mathrm{g,c}}(s)}{E_{\omega}(s)} = \frac{K_{\mathrm{p}} s + K_{\mathrm{i}}}{s}, \tag{11}$$

and in series with $G_1(s)$, one obtains the loop transfer

$$\begin{aligned} L_1(s) &= G_1(s) C(s) \\ &= \frac{-1}{J \bar{\omega}_{\mathrm{r}}} \frac{\left(K_{\mathrm{p}} s + K_{\mathrm{i}} \right) \left(s + K_{\mathrm{U}} \left(V - \lambda^* / R \left(Q - \hat{Q} \right) \right) \right)}{s \left(s - \left(T + \bar{P}_{\mathrm{g}} / \bar{\omega}_{\mathrm{r}}^2 \right) / J \right) \left(s + K_{\mathrm{U}} V \right)}, \end{aligned} \tag{12}$$

and by closing the loop around the loop transfer in- and output e_{ω}, the following single-input single-output (SISO) transfer function is obtained

$$H(s) = \frac{E_{\mathrm{P}}(s)}{\mathcal{P}_{\mathrm{g,e}}(s)} = \frac{G_2(s)}{1 - L_1(s)} = \frac{-\left(Q - \hat{Q} \right) s^2}{J \left(\Xi_1 + \Xi_2 \right)}, \tag{13}$$

in which $\Xi_1 = \bar{\omega}_{\mathrm{r}} s \left(s - \left(T + \bar{P}_{\mathrm{g}} / \bar{\omega}_{\mathrm{r}}^2 \right) / J \right) \left(s + K_{\mathrm{U}} V \right)$ and $\Xi_2 = \left(1 / J \right) \left(K_{\mathrm{p}} s + K_{\mathrm{i}} \right) \left(s + K_{\mathrm{U}} \left(V - \lambda^* / R \left(Q - \hat{Q} \right) \right) \right)$ are used to make the expression more compact.

The key transfer for the development of an active learning strategy is the closed-loop transfer function $H(s)$ between the input $\mathcal{P}_{\mathrm{g,e}}(s)$ and output $E_{\mathrm{P}}(s)$, as its overall gain diminishes under increasing model certainty. This property is a key-enabling factor for the development of the learning algorithm proposed in this work.

III. MODEL UNCERTAINTY

This section describes how model uncertainty is included in the proposed framework, and illustrates the effect on the frequency response of $H(s)$. Furthermore, an analysis and illustrative example is given on the convex properties in its magnitude response.

A. Definition of model uncertainty

Under Assumption 2 and 3, this paper considers model uncertainty as a multiplicative degradation function acting on the ideal (modeled) aerodynamic rotor properties, and is defined as

$$C_{\mathrm{P}}(\lambda) \triangleq \Gamma(\lambda) C_{\mathrm{P}}^{\diamond}(\lambda). \tag{14}$$

Note that the degradation function $\Gamma(\lambda)$ is a function of λ and is unknown in real-world scenarios. Similarly, the ideal power coefficient data included in and used for the overall control system is obtained by multiplication of the estimated degradation function with the ideal aerodynamic rotor properties:

$$\hat{C}_{\mathrm{P}}(\hat{\lambda}) \triangleq \hat{\Gamma}(\alpha, \hat{\lambda}) C_{\mathrm{P}}^{\diamond}(\hat{\lambda}), \tag{15}$$

and the estimated degradation function is defined as

$$\hat{\Gamma}(\alpha, \hat{\lambda}) \triangleq \alpha \gamma(\hat{\lambda}), \tag{16}$$

where $\gamma(\hat{\lambda}) : \mathbb{R} \to \mathbb{R}$ is the degradation profile with $\alpha \in \mathbb{R}^{+}$ being its magnitude scaling. This paper provides a proof of concept for the proposed novel learning algorithm. As will become apparent later, due to the ill-conditioning of the control scheme [9] currently only degradation functions parameterized by a single variable can be compensated for.

Furthermore, by equating the steady-state result of aerodynamic rotor power and its estimate, i.e. $P_{\mathrm{r}} = \hat{P}_{\mathrm{r}}$, respectively defined by (2) and (5), and substituting the uncertainty expressions (14) and (15) one obtains

$$\hat{U}^3 = U^3 \frac{C_{\mathrm{P}}(\lambda)}{\hat{C}_{\mathrm{P}}(\hat{\lambda})} = U^3 \frac{\Gamma(\lambda)}{\hat{\Gamma}(\alpha, \hat{\lambda})} \frac{C_{\mathrm{P}}^{\diamond}(\lambda)}{C_{\mathrm{P}}^{\diamond}(\hat{\lambda})}. \tag{17}$$

As shown, an accurate estimate of the actual REWS can only be made when $C_{\mathrm{P}}(\lambda) = \hat{C}_{\mathrm{P}}(\hat{\lambda})$. In the proposed uncertainty definition framework, this consequently means that a consistent estimate of Γ by $\hat{\Gamma}$ is required, and the actual aerodynamic characteristics are successfully modeled when $\Gamma(\lambda)/\hat{\Gamma}(\alpha, \hat{\lambda}) = 1 \,\forall\, \left(\lambda = \hat{\lambda}\right)$.

B. Convex properties of the proposed transfer function

The closed-loop transfer function $H(s)$ defined in (13) possesses a DC gain term as the difference between the actual and estimated partial derivative of the rotor power with respect to the rotor speed (respectively indicated by Q and $\hat{Q}$). The difference between those terms and, in turn, the magnitude of the frequency response of $H(s)$ nullify whenever the turbine model information matches with the actual aerodynamic properties. This remarkable (convex) property of the transfer function's magnitude response is further analyzed in this section.

The partial derivative represented by Q is defined as

$$\frac{\partial P_{\mathrm{r}}}{\partial \omega_{\mathrm{r}}} = \frac{1}{2} \rho A R U^2 \frac{\partial C_{\mathrm{P}}}{\partial \lambda}, \tag{18}$$

and a similar expression is obtained for its estimate $\hat{Q}$ based on (5). Upon closer inspection of the difference term and under Assumption 2, one obtains the following relation:

$$\frac{\partial P_{\mathrm{r}}}{\partial \omega_{\mathrm{r}}} - \frac{\partial \hat{P}_{\mathrm{r}}}{\partial \omega_{\mathrm{r}}} = \frac{1}{2} \rho A R \left(U^2 \frac{\partial C_{\mathrm{P}}}{\partial \lambda} - \hat{U}^2 \frac{\partial \hat{C}_{\mathrm{P}}}{\partial \hat{\lambda}} \right), \tag{19}$$

and the above-given expression nullifies whenever

$$U^2 \frac{\partial C_{\mathrm{P}}}{\partial \lambda} = \hat{U}^2 \frac{\partial \hat{C}_{\mathrm{P}}}{\partial \hat{\lambda}}. \tag{20}$$

The proposed learning scheme is based on the idea to equate these two terms, minimizing the transfer $H(s)$. Using (17), a convex minimization problem is formalized as

$$\underset{\hat{C}_{\mathrm{P}},\ \frac{\partial \hat{C}_{\mathrm{P}}}{\partial \hat{\lambda}}}{\arg\min} \left| \frac{1}{C_{\mathrm{P}}^{(2/3)}(\lambda)} \frac{\partial C_{\mathrm{P}}}{\partial \lambda}(\lambda) - \frac{1}{\hat{C}_{\mathrm{P}}^{(2/3)}(\hat{\lambda})} \frac{\partial \hat{C}_{\mathrm{P}}}{\partial \hat{\lambda}}(\hat{\lambda}) \right|. \tag{21}$$

It is recognized that in (21), the first term consists out of real-world characteristic turbine properties as a function of the turbine operational state and environmental conditions, whereas the second term contains their modeled and estimated representations.

One can already recognize that the individual terms making up the product of the real-world turbine properties cannot be uniquely estimated; only their product is known. Earlier work [9] describes a similar type of ill-conditioning and reveals that inaccurate C_{P}-information in the wind speed estimator is counteracted by a biased wind speed estimate $\hat{U}$, as also concluded from (17).

For solving the minimization problem in (21), one can either calibrate the modeled power coefficient information, its gradient, or a combination of both. Therefore, in its current form, the minimization is underdetermined, and one should take into account the following additional observations in solving the minimization problem of (21):

1) The problem can be minimized by taking the power coefficient gradient as a decision variable, which does not have an effect on the correctness of the estimated REWS.
2) Setting the tip-speed ratio reference to track the maximum power coefficient results in an estimated power coefficient gradient being equal to 0. This situation adds another layer of complexity of the underdetermined minimization problem, as an infinite number of solutions exist. This point is further outlined in Section III-C.

Because of the above-mentioned reasons and observations, and according to the current stage of this research, for now, assumptions have to be made on types of uncertainty that the proposed scheme can correct for. This is the reason for defining the estimated degradation function in (16) as a multiplication between an a priori known degradation profile $\gamma(\hat{\lambda})$ and its unknown scaling factor α.

C. Learning limitations at the maximum power-coefficient

This section describes the remarkable property of the algorithm being unable to learn the actual aerodynamic characteristics when operating the turbine at the tip-speed ratio $\lambda^* = \arg\max_{\hat{\lambda}} \hat{C}_{\mathrm{P}}(\hat{\lambda})$, maximizing steady-state power capture.

The above described is seen by substituting the derivatives of (14) and (15) with respect to their tip-speed ratio

arguments in (20), resulting in

$$U^2\left(\frac{\partial\Gamma}{\partial\lambda}(\lambda)C_{\mathrm{P}}^{\diamond}(\lambda)+\Gamma(\lambda)\frac{\partial C_{\mathrm{P}}^{\diamond}}{\partial\lambda}(\lambda)\right)= \hat{U}^2\left(\frac{\partial\hat{\Gamma}}{\partial\lambda}(\alpha,\hat{\lambda})C_{\mathrm{P}}^{\diamond}(\lambda)+\hat{\Gamma}(\alpha,\hat{\lambda})\frac{\partial C_{\mathrm{P}}^{\diamond}}{\partial\lambda}(\hat{\lambda})\right). \quad (22)$$

Now by assuming that the actual degradation function is a constant ($\Gamma = C$), one can disregard the first terms at the left- and right-hand side of the equation, and by recognizing that $\partial\hat{C}_{\mathrm{P}}/\partial\hat{\lambda}\,(\lambda^*) = 0$, then (22) reduces to

$$U^2\left(\Gamma(\lambda)\frac{\partial C_{\mathrm{P}}^{\diamond}}{\partial\lambda}(\lambda)\right)=0, \quad (23)$$

which eliminates the algorithm's ability to learn $\hat{\Gamma}(\alpha,\hat{\lambda})$.

To solve this problem, the turbine tip-speed ratio set point should be relocated – during the learning phase – from the power-coefficient maximizing location λ^* to a temporary set point location $\tilde{\lambda}^*$ where the gradient is nonzero, such that $\partial C_{\mathrm{P}}^{\diamond}/\partial\lambda\,(\tilde{\lambda}^*) \neq 0$. Then, for the considered case, the following equality holds

$$U^2\Gamma(\lambda)\frac{\partial C_{\mathrm{P}}^{\diamond}}{\partial\lambda}(\lambda)=\hat{U}^2\hat{\Gamma}(\alpha,\tilde{\lambda}^*)\frac{\partial C_{\mathrm{P}}^{\diamond}}{\partial\lambda}(\tilde{\lambda}^*). \quad (24)$$

D. Analyzing the convex transfer properties

In this section, the effect of model uncertainty on $H(s)$ is analyzed. For evaluation and illustration of the transfer function, the NREL 5-MW reference wind turbine is considered [4]. For purposes of the learning algorithm, the turbine operates at a nonoptimal TSR set point of $\bar{\lambda}^* = 9.5$, whereas the controller and estimator gains are constant for all operating conditions at $K_{\mathrm{p}} = 4.57\cdot10^5$, $K_{\mathrm{i}} = 4.57\cdot10^4$, and $K_{\mathrm{U}} = 1.67\cdot10^{-7}$. The degradation function – acting on the actual aerodynamic turbine properties – are analyzed for the set of constant multiplicative factors $\Gamma = \{0.85,\ 0.95,\ 0.99,\ 1.2\}$. Note that the actual tip-speed ratio operating point $\bar{\lambda}$ deviates from the requested set point with increasing uncertainty, as a result of the inherent ill-conditioning of the considered controller scheme [9]. The resulting steady-state operating points are obtained for each uncertainty level and are used for evaluation of $H(s)$.

Fig. 2 shows the set of frequency responses $H(\mathrm{j}\omega)$, evaluated at the above-given uncertainty levels. Furthermore, for interpretation of this figure, the characteristic equation $D(s)$ in $H(s) = N(s)/D(s)$ for a nondegraded wind turbine is derived (i.e., $\hat{Q} = Q$):

$$D(s)|_{\hat{Q}=Q} = \bar{\omega}_{\mathrm{r}}\left(s^2+\frac{1}{J\bar{\omega}_{\mathrm{r}}}\left(K_{\mathrm{p}}-\frac{\bar{P}_{\mathrm{g}}}{\bar{\omega}_{\mathrm{r}}}-T\bar{\omega}_{\mathrm{r}}\right)s+\frac{K_{\mathrm{i}}}{J\bar{\omega}_{\mathrm{r}}}\right)(s+K_{\mathrm{U}}V). \quad (25)$$

The reason for the notation of the above is that the numerator $N(s) = 0$ for the considered case. While the characteristic equation in (25) does not exactly resemble the presented frequency response trajectories in the Fig. 2, the equation is still useful to recognize of some remarkable properties of the transfer $H(s)$:

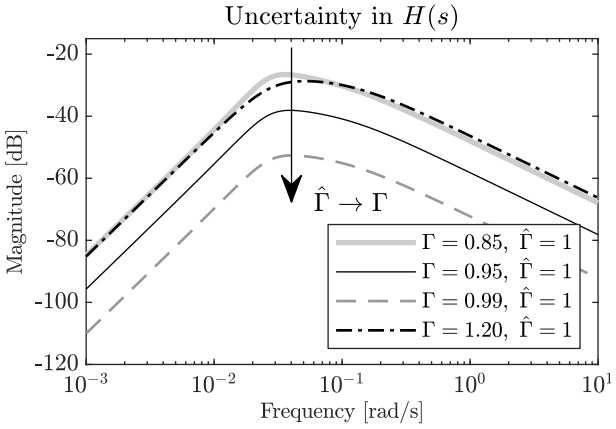

Fig. 2. Bode plot of $H(s)$ for the set of multiplicative (constant factor) uncertainties $\Gamma = \{0.85,\ 0.95,\ 0.99,\ 1.2\}$, and $\hat{\Gamma} = 1$ for all cases. The maximum magnitude response frequency depends on specific operating conditions, rotor structural properties, and controller gains. It is shown that the magnitude response diminishes for $\hat{\Gamma} \to \Gamma$. The case for $\Gamma = 1.0$ is not displayed as its transfer is nonexistent.

- The transfer has a zero DC gain as a result of the double pure zero in $H(s)$.
- The overall magnitude diminishes as $\hat{\Gamma} \to \Gamma$.
- Whenever the degradation is under- or overestimated, the sign of the transfer flips (phase plot omitted).
- The magnitude response shows a maximum gain in a very specific frequency interval, induced by the second-order term in $D(s)$. The following can be said on its natural frequency and damping:
  - The location of the natural frequency is induced by the TSR tracking controller integral gain K_{i}, the operating point and other turbine properties.
  - The damping is determined by the controller proportional gain K_{p}, the operating point and other turbine properties.

The next section elaborates on the development of a continuous learning algorithm benefiting from the convex properties.

IV. THE ACTIVE LEARNING ALGORITHM

Unlike most other learning algorithms, the proposed approach in this section exploits the convex dynamic properties of the turbine control scheme, without the need for a wind speed measurement. The goal of the algorithm is to correct the wind speed estimator internal model in terms of the power coefficient information. This section first presents a concise overview of the learning approach, after which the algorithm is further detailed.

A. Overview of the learning algorithm

As the learning strategy aims at minimizing the periodic excitation signal present in the output e_{P}, various learning approaches can be derived accomplishing this goal. The approach proposed in the paper is an excitation-demodulation based learning approach, of which a schematic block diagram is presented in Fig. 3. The scheme shows that by periodically exciting $P_{\mathrm{g,e}}$ with a single sinusoid at frequency ω_{L}, the

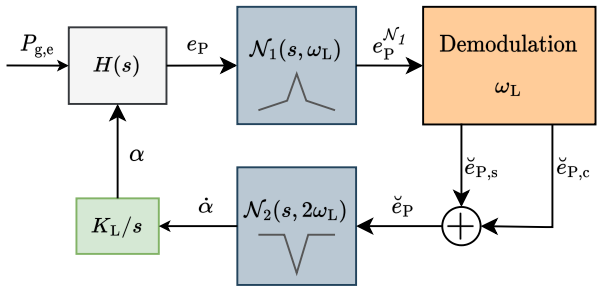

Fig. 3. The closed-loop system $H(s)$ is subject to a single frequency dynamic excitation signal at $P_{\mathrm{g,e}}$. Because the system is assumed to show linear characteristics around an operating point, the output signal e_{P} possesses a magnitude-scaled and phase-shifted version of the excitation signal. To single out that frequency content, the inverted notch $\mathcal{N}_1$ is employed, of which its resulting signal is subject to a demodulation operation. This operation moves the dynamic frequency content to a combined DC and a higher-harmonic contribution, of which the latter is attenuated by notch filter $\mathcal{N}_2$. The resulting signal consists of a dominant DC component, that represents the system magnitude transfer, and is minimized in realtime by finding the correct scaling factor α.

output signal e_{P} is subsequently filtered, demodulated and numerically integrated. The result after integration is α to scale the a priori known degradation profile $\gamma(\hat{\lambda})$ as in (16). Whenever an α is found such that $\Gamma(\lambda) = \hat{\Gamma}(\hat{\lambda})$, the gain of $H(s)$ nullifies.

B. Derivation of the learning algorithm

The closed-loop system $H(s)$ is excited with the single-frequency periodic signal

$$P_{\mathrm{g,e}}(t) = A_{\mathrm{P}} \sin(\omega_{\mathrm{L}} t), \tag{26}$$

where A_{P} and ω_{L} are the excitation amplitude and frequency, respectively. From the linear system theory, it follows that the output is a magnitude-scaled and phase-shifted version of the excitation signal, such that

$$e_{\mathrm{P}}(t) = A_{\mathrm{e}} \sin(\omega_{\mathrm{L}} t + \psi_{\mathrm{H}}), \tag{27}$$

where $A_{\mathrm{e}} = A_{\mathrm{P}} \, |H(\mathrm{j}\omega_{\mathrm{L}})|$ being the output amplitude of the resulting excitation signal, with a phase shift $\psi_{\mathrm{H}} = \angle H(\mathrm{j}\omega_{\mathrm{L}})$ representing the phase loss in the system at the excitation frequency. Next, the system response at the excitation frequency is isolated by the use of the following (inverted) notch filter with $+1/-1$ slopes to the left and right side of its natural frequency:

$$\mathcal{N}_1(s,\omega_{\mathrm{L}}) = \frac{E_{\mathrm{P}}(s)}{E_{\mathrm{P}}^{\mathcal{N}_1}(s)} = K \frac{s}{s^2 + 2\zeta\omega_{\mathrm{L}} s + \omega_{\mathrm{L}}^2}, \tag{28}$$

in which ζ is the damping ratio, and the gain $K = 2\zeta\omega_{\mathrm{L}}$ for a unity gain at the fundamental frequency of the filter. The resulting time-domain output signal is

$$e_{\mathrm{P}}^{\mathcal{N}_1}(t) = A_{\mathrm{e}} \sin(\omega_{\mathrm{L}} t + \psi_{\mathrm{HN}}), \tag{29}$$

and is subsequently subject to a signal demodulation operation, to transfer the frequency response content at ω_{L} to a static DC contribution. In the time-domain, demodulation comes down to the following operation

$$\begin{aligned} \check{e}_{\mathrm{P}}(t) &= e_{\mathrm{P}}^{\mathcal{N}_1}(t)\Big(\sin(\omega_{\mathrm{L}} t + \psi_{\mathrm{D}}) + \cos(\omega_{\mathrm{L}} t + \psi_{\mathrm{D}})\Big), \\ &= \frac{A_{\mathrm{e}}}{2} + \frac{A_{\mathrm{e}}}{2}\Big(\sin\big(2(\omega_{\mathrm{L}} t + \psi_{\mathrm{D}})\big) - \cos\big(2(\omega_{\mathrm{L}} t + \psi_{\mathrm{D}})\big)\Big), \end{aligned} \tag{30}$$

and the above-given derivation only holds when $\psi_{\mathrm{D}} = \psi_{\mathrm{HN}}$, where ψ_{D} is a phase-offset tuning variable to compensate for the phase loss ψ_{HN} caused by dynamic operations and system delays. The correct tuning of ψ_{D} increases the convergence performance of the considered learning scheme [17]. As shown in (30), the resulting signal $\check{e}_{\mathrm{P}}$ now consists of a linear combination of a steady-state offset $A_{\mathrm{e}}/2$ with a periodic contribution at $2\omega_{\mathrm{L}}$. This signal, subject to a notch filter at $2\omega_{\mathrm{L}}$, is given by

$$\mathcal{N}_2(s,2\omega_{\mathrm{L}}) = \frac{\dot{\mathcal{A}}(s)}{\check{E}_{\mathrm{P}}(s)} = \frac{s^2 + 2\zeta_1(2\omega_{\mathrm{L}})s + (2\omega_{\mathrm{L}})^2}{s^2 + 2\zeta_2(2\omega_{\mathrm{L}})s + (2\omega_{\mathrm{L}})^2}, \tag{31}$$

where $\mathcal{A}(s)$ is the Laplace representation of the time-domain signal α, and ζ_1, ζ_2 are the respective numerator and denominator damping coefficients. Lastly, the magnitude scaling of the degradation profile is numerically integrated with learning gain K_{L}. The scaling factor α is a direct calibration parameter into the nonlinear closed-loop system to the estimated degradation function in (16). Because of the convex and sign altering properties of the considered transfer, the above-described learning scheme converges.

V. RESULTS

This section showcases the working principles and performance of the proposed learning algorithm by multiple simulation case studies. The simulation environment entails a nonlinear first-order wind turbine model representing the NREL 5-MW reference turbine, subject to the WSE-TSR tracking control scheme according to Fig. 1. Only the partial-load region is considered (Assumption 1), by subjecting the turbine to constant and turbulent ($\mathrm{TI} = 3\,\%$) wind profiles with a mean wind speed of $\bar{U} = 7$ m/s.

The chosen turbulence intensity results in satisfactory convergence of the algorithm; further research needs to be performed to provide robust learning performance for lower signal-to-noise (SNR) ratios. The parameters for the learning algorithm are the learning gain $K_{\mathrm{L}} = -0.5 \cdot 10^{-9}$ m s^{-1} W^{-1}, demodulation phase offset $\psi_{\mathrm{D}} = 130$ deg, power excitation amplitude and frequency $A_{\mathrm{P}} = 500$ kW and $\omega_{\mathrm{L}} = 0.02$ Hz, and the tip-speed ratio set point for learning $\lambda^* = 9.5$.

A constant-factor degradation function $\Gamma = 0.85$ is taken, degrading the rotor power coefficient characteristics with respect to that of the actual turbine. This degradation case is considered for all simulation cases and is aimed for correction by $\hat{\Gamma}(\alpha, \gamma = 1) = \alpha$, with $\alpha_0 = 1.0$ as an initial value. The baseline case $\Gamma = 1.0$, shown in the same figure, indicates there is no degradation on the power coefficient, i.e., $C_{\mathrm{p}} = C_{\mathrm{p}}^{\diamond}$.

Fig. 4 shows the results for several runs of the learning progress for the considered wind profiles. For the constant

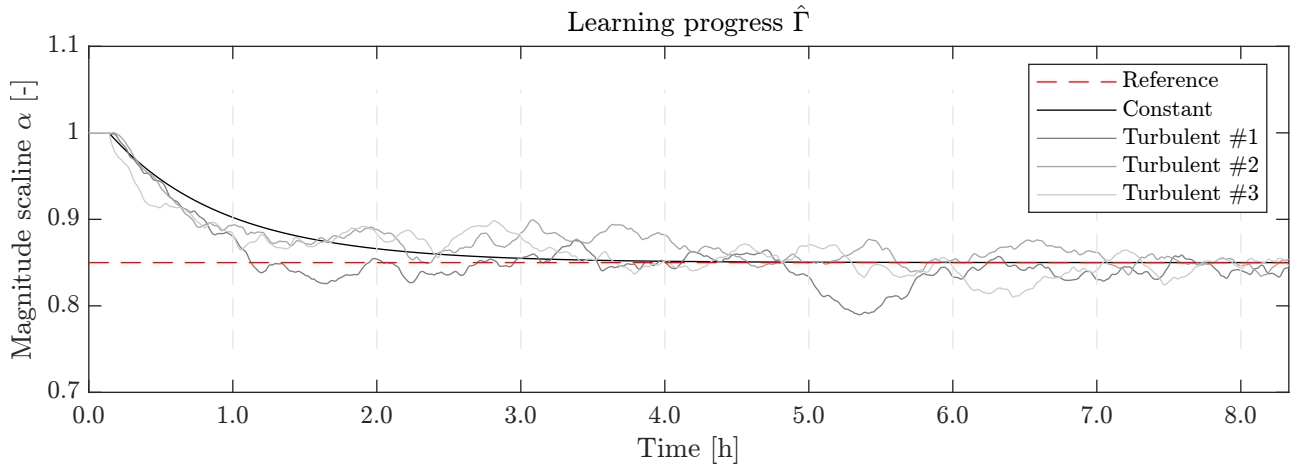

Fig. 4. The learning progress is illustrated for an actual aerodynamic performance constant-factor degradation scenario represented by $\Gamma = 0.85$. The two learning scenarios considered are subject to a constant wind profile and three distinct realizations of realistic turbulent wind fields ($\mathrm{TI} = 3\,\%$). The figure shows a reference for the estimated degradation function $\hat{\Gamma} = \alpha = 0.85$ that is to be discovered by the scheme by the red dashed line. For the constant wind speed, the scheme is seen to converge to the exact degradation magnitude correction factor. For the turbulent cases, the algorithm is also shown to converge to the correct value, however the trajectories show an increased variance around the optimum. Although the simulations are run for an extended period of time to indicate convergence, the algorithms is seen to converge on a time scale of hours.

wind profile, the algorithm accurately finds the actual degradation factor. For the different turbulent realizations, the degradation magnitude is found correctly, however, variance is observed around the optimal value. Convergence is concluded empirically based on comparison with the reference degradation factor α. Furthermore, the three distinct realizations of the turbulent case remain *close* to the actual optimum value for extended time periods. It is also recognized that the speed of the algorithm is on the time scale of hours, which makes the learning scheme most suitable for learning long-term degradation scenarios such as leading-edge erosion.

VI. CONCLUSIONS

This paper presents a novel learning algorithm for calibrating the internal model employed in modern and advanced wind turbine controllers. An excitation-based learning algorithm is proposed for the first time without the need for wind speed measurements. Considering a specific input/output pair of the wind turbine control scheme in a linear analysis framework demonstrates a convex property, which is a key-enabling factor for the development of a learning algorithm. The algorithm thereby exploits the structure and dynamics of the combined tip-speed ratio tracking and wind speed estimation control scheme. Preliminary studies show its ability to discover and correct for a constant-factor power coefficient degradation case under ideal constant and more realistic turbulent wind conditions.

Future work will focus on the further development of the learning algorithm to alleviate constraints on the degradation profiles that can be compensated for, thereby increasing the practical applicability. Furthermore, analysis and improvement of the signal-to-noise ratio between the excitation signal and the wind disturbance input will be considered for faster convergence, reduced excitation magnitudes, and the ability to learn in even more realistic environmental conditions.

REFERENCES

[1] I. Komusanac, G. Brindley, D. Fraile, *et al.*, "Wind energy in Europe - 2021 Statistics and the outlook for 2022-2026," Tech. Rep., 2022.

[2] T. Burton, N. Jenkins, D. Sharpe, *et al.*, *Wind energy handbook*. Chichester, United Kingdom: John Wiley & Sons, 2001.

[3] P. Veers, K. Dykes, E. Lantz, *et al.*, "Grand challenges in the science of wind energy," *Science*, vol. 366, no. 6464, 2019.

[4] J. Jonkman, S. Butterfield, W. Musial, *et al.*, "Definition of a 5-MW reference wind turbine for offshore system development," National Renewable Energy Laboratory (NREL), Tech. Rep., 2009.

[5] E. A. Bossanyi, "The design of closed loop controllers for wind turbines," *Wind Energy*, no. 3, pp. 149–163, 2000.

[6] N. J. Abbas, D. S. Zalkind, L. Pao, *et al.*, "A reference open-source controller for fixed and floating offshore wind turbines," *Wind Energy Science*, vol. 7, no. 1, pp. 53–73, 2022.

[7] M. N. Soltani, T. Knudsen, M. Svenstrup, *et al.*, "Estimation of rotor effective wind speed: A comparison," *IEEE Transactions on Control Systems Technology*, vol. 21, no. 4, pp. 1155–1167, 2013.

[8] K. Franke and A. Albers, "Poster: Power curve uncertainty of rotor equivalent wind speed," in *WindEurope Summit 2016*, September 2016.

[9] L. Brandetti, Y. Liu, S. P. Mulders, *et al.*, "On the ill-conditioning of the combined wind speed estimator and tip-speed ratio tracking control scheme," *Journal of Physics: Conference Series*, 2022.

[10] L. J. Fingersh and P. Carlin, "Results from the NREL variable-speed test bed," in *Proc. 17th ASME Wind Energy Symp.*, 1999, pp. 233–237.

[11] K. E. Johnson, L. Y. Pao, M. J. Balas, *et al.*, "Control variable-speed wind turbines: Standard and adaptive techniques for maximizing energy capture," *IEEE Control Systems*, vol. 26, 2006.

[12] W. H. Lio, A. Li, and F. Meng, "Real-time rotor effective wind speed estimation using Gaussian process regression and Kalman filtering," *Renewable Energy*, vol. 169, pp. 670–686, 2021.

[13] J. D. M. De Kooning, L. Gevaert, J. Van de Vyver, *et al.*, "Online estimation of the power coefficient versus tip-speed ratio curve of wind turbines," in *IECON 2013 - 39th Annual Conference of the IEEE Industrial Electronics Society*, 2013, pp. 1792–1797.

[14] J. Dai, D. Liu, L. Wen, *et al.*, "Research on power coefficient of wind turbines based on SCADA data," *Renewable Energy*, 2016.

[15] R. Ortega, F. Mancilla-David, and F. Jaramillo, "A globally convergent wind speed estimator for wind turbine systems," *International Journal of Adaptive Control and Signal Processing*, vol. 27, pp. 413–425, 2013.

[16] Y. Liu, A. K. Pamososuryo, R. M. Ferrari, *et al.*, "The Immersion and Invariance wind speed estimator revisited and new results," *IEEE Control Systems Letters*, vol. 6, pp. 361–366, 2022.

[17] J.-S. Deschênes, "Demodulation considerations in extremum seeking control loops," in *American Control Conference (ACC)*, 2012.